

## **Mathematical modeling of space-time variations in acoustic transmission and scattering from schools of swim bladder fish (FY11 Annual Report)**

Christopher Feuillade  
Pontificia Universidad Católica de Chile  
Facultad de Física  
Av. Vicuña Mackenna 4860  
Santiago, Chile  
phone: +56 2 354 4800 fax: +56 2 354 4491 email: [chris.feuilleade@gmail.com](mailto:chris.feuilleade@gmail.com)

Award Number: N00014-111-0161

### **LONG-TERM GOALS**

The goal is the development of a time-domain acoustical method for investigating the spatial and temporal stochastic variations in fish density within fish schools, and thereby study the statistical fluctuations in the scattering of sound from these objects.

### **OBJECTIVES**

The objective of this research is to develop a complete time-domain theory of acoustic scattering from, and propagation through, schools of swim bladder fish at and near the swim bladder resonance frequency, including multiple scattering and coherent interaction effects between the individual fish. This should then lead to a prescriptive capability for modeling the evolution of sound pulses as they are scattered from, and pass through, fish schools. Subsequently, it should be possible to identify discrete segments of the signal with different sections of the fish school, and enable an enhanced understanding of signal scattering, and extinction, by the school, and the fluctuations in these properties.

### **APPROACH**

The personnel participating in this work at the present time are: Principal Investigator: Christopher Feuillade - Ph. D. (Physics), Manchester, UK, 1977. (Visiting Professor, Pontificia Universidad Católica de Chile); Assistant: Maria Paz Raveau Morales - Civil Engineer in Sound and Acoustics - INACAP, Chile, 2009. (Doctoral student, Pontificia Universidad Católica de Chile)

A methodology for approaching this problem is available through the application of self-consistent mathematical techniques (see Ref 1). The formalism used is based upon the solution of sets of coupled differential equations, and incorporates a verified swim bladder scattering kernel (Ref. 2) for an individual fish. All orders of multiple scattering interactions between the fish are included, and the aggregate scattering field calculated by coherent summation.

(a) Steady-state solution: Near the swim bladder resonance frequency, the azimuthal scattering

Report Documentation Page				Form Approved OMB No. 0704-0188	
Public reporting burden for the collection of information is estimated to average 1 hour per response, including the time for reviewing instructions, searching existing data sources, gathering and maintaining the data needed, and completing and reviewing the collection of information. Send comments regarding this burden estimate or any other aspect of this collection of information, including suggestions for reducing this burden, to Washington Headquarters Services, Directorate for Information Operations and Reports, 1215 Jefferson Davis Highway, Suite 1204, Arlington VA 22202-4302. Respondents should be aware that notwithstanding any other provision of law, no person shall be subject to a penalty for failing to comply with a collection of information if it does not display a currently valid OMB control number.					
1. REPORT DATE <b>SEP 2011</b>		2. REPORT TYPE		3. DATES COVERED <b>00-00-2011 to 00-00-2011</b>	
4. TITLE AND SUBTITLE <b>Mathematical modeling of space-time variations in acoustic transmission and scattering from schools of swim bladder fish (FY11 Annual Report)</b>				5a. CONTRACT NUMBER	
				5b. GRANT NUMBER	
				5c. PROGRAM ELEMENT NUMBER	
6. AUTHOR(S)				5d. PROJECT NUMBER	
				5e. TASK NUMBER	
				5f. WORK UNIT NUMBER	
7. PERFORMING ORGANIZATION NAME(S) AND ADDRESS(ES) <b>Pontificia Universidad Catolica de Chile,Facultad de F&amp;#305;sica,Av. Vicuna Mackenna 4860,Santiago, Chile,</b>				8. PERFORMING ORGANIZATION REPORT NUMBER	
9. SPONSORING/MONITORING AGENCY NAME(S) AND ADDRESS(ES)				10. SPONSOR/MONITOR'S ACRONYM(S)	
				11. SPONSOR/MONITOR'S REPORT NUMBER(S)	
12. DISTRIBUTION/AVAILABILITY STATEMENT <b>Approved for public release; distribution unlimited</b>					
13. SUPPLEMENTARY NOTES					
14. ABSTRACT					
15. SUBJECT TERMS					
16. SECURITY CLASSIFICATION OF:			17. LIMITATION OF ABSTRACT <b>Same as Report (SAR)</b>	18. NUMBER OF PAGES <b>8</b>	19a. NAME OF RESPONSIBLE PERSON
a. REPORT <b>unclassified</b>	b. ABSTRACT <b>unclassified</b>	c. THIS PAGE <b>unclassified</b>			

distribution of an individual fish is practically spherically symmetric, and this has led to the development of “bubble-like” swim bladder models, where the resonance behavior is described by a “mass-spring” type differential equation, i.e.,

$$m\ddot{v} + b\dot{v} + \kappa v = -Pe^{i\omega t} \quad , \quad (1)$$

where  $v$  is the differential volume (i.e., the difference between the instantaneous and equilibrium bubble volumes). The coefficient  $m(= \rho/4\pi a)$  is termed the inertial “mass” of the bubble, where  $a$  is the bubble radius and  $\rho$  the water density; and  $\kappa(= 3\gamma P_A/4\pi a^3)$  is the “adiabatic stiffness”, where  $\gamma$  is the ratio of gas specific heats and  $P_A$  the ambient pressure. The variables  $P$  and  $\omega$  represent the amplitude and frequency respectively of the periodic external pressure field, and the coefficient  $b$  describes the damping of the bubble motion. In the school model solution,  $b$  is replaced by a factor corresponding to the damping predicted by a suitable swim bladder model for the species and depth location of the fish under examination.

If a harmonic steady state solution of (1) of the form  $v = \bar{v}e^{i\omega t}$  is assumed, substitution gives the resonance response

$$\bar{v} = \frac{-P}{\kappa - \omega^2 m + i\omega b} = \frac{(-P/m\omega^2)}{(\omega_0^2/\omega^2) - 1 + i(b/m\omega)} \quad , \quad (2)$$

where  $\omega_0 = \sqrt{\kappa/m} = \sqrt{3\gamma P_A/\rho}$  is the resonance frequency. Equation (2) describes a Lorentzian resonance response. The imaginary component  $(b/m\omega)$  in the denominator can be identified with a damping constant  $\delta$  for the bubble, consisting of radiative, viscous and thermal terms, i.e.,

$$(b/m\omega) = \delta = \delta_r + \delta_v + \delta_t. \quad (3)$$

At resonance the damping constant is equivalent to the reciprocal of the “quality factor”  $Q$ , so that

$$\delta_R = \delta_{Rr} + \delta_{Rv} + \delta_{Rt} = \frac{1}{Q}. \quad (4)$$

In the theory of resonant acoustic scattering by fish swim bladders developed by Love (Ref. 2), the quantity  $\delta$  is replaced by a factor  $(\omega_0/\omega H)$ . The frequency dependent parameter  $H$  (which is equal to  $Q$  at resonance) also consists of three components, which are combined as follows

$$\frac{1}{H} = \frac{1}{H_r} + \frac{1}{H_v} + \frac{1}{H_t}. \quad (5)$$

In the case of fishes, the damping due to thermal conductivity effects is generally negligible compared to radiative and viscous damping. The values of  $H_r$  and  $H_v$  are given by

$$H_r = \frac{\omega_0 c}{\omega^2 a} \quad ; \quad H_v = \frac{\omega_0 \rho a^2}{2\xi} \quad (6)$$

where  $\xi$  is the viscosity of fish flesh surrounding the bladder. The difference between water and fish flesh densities is generally very small and may be neglected.

(2) Steady-state solution of a school of fish: When a swim bladder is ensonified by an external field, it scatters sound. The acoustic field reradiated by the bladder is predominantly monopolar and isotropic, and the pressure field at radial distance  $r$  due to scattering is given by

$$p(r) = \frac{\rho e^{-ikr}}{4\pi r} \ddot{v} \quad (7)$$

If we consider an external field driving an ensemble of  $N$  interacting swim bladders. The total field incident on any one of the bladders is the sum of the external field and the scattered fields from all of the others. The response of a whole ensemble of fish (all of them different from each other) may be represented by a set of coupled differential equations as follows:

$$\begin{aligned}
m_1 \ddot{v}_1 + b_1 \dot{v}_1 + \kappa_1 v_1 &= -P_1 e^{i(\omega t + \phi_1)} - \sum_{j \neq 1}^N \frac{\rho e^{-ikr_{j1}}}{4\pi r_{j1}} \ddot{v}_j \\
&\dots\dots\dots \\
m_n \ddot{v}_n + b_n \dot{v}_n + \kappa_n v_n &= -P_n e^{i(\omega t + \phi_n)} - \sum_{j \neq n}^N \frac{\rho e^{-ikr_{jn}}}{4\pi r_{jn}} \ddot{v}_j \quad . \\
&\dots\dots\dots \\
m_N \ddot{v}_N + b_N \dot{v}_N + \kappa_N v_N &= -P_N e^{i(\omega t + \phi_N)} - \sum_{j=1}^{N-1} \frac{\rho e^{-ikr_{jN}}}{4\pi r_{jN}} \ddot{v}_j
\end{aligned} \tag{8}$$

Here,  $P_n$  and  $\phi_n$  are the amplitude and phase respectively of the external field experienced by the  $n$ th bladder, and  $r_{jn}$  is the radial distance from the center of the  $n$ th bladder to the center of the  $j$ th bladder. The quantities  $b_n$  in these equations incorporate the damping factors from the Love swim bladder model of Ref. 2. The LHS of these equations describe the motions of each of the  $N$  bubbles [as on the LHS of eq. (1)], and the RHS give the total aggregate field acting on each one of them.

Harmonic “steady-state” solutions of these coupled equations were found by substituting  $v_n = \bar{v} e^{i\omega t}$  etc. in (8). This leads to a matrix equation which may be written  $\mathbf{M}\mathbf{v} = \mathbf{p}$ ; where  $\mathbf{v} = \{v_1, \dots, v_n, \dots, v_N\}$  and  $\mathbf{p} = \{-P_1 e^{i\phi_1}, \dots, P_n e^{i\phi_n}, \dots, P_N e^{i\phi_N}\}$  are column vectors containing the steady state volume oscillation amplitudes and external fields respectively for the individual bladders, and  $\mathbf{M}$  is an  $N \times N$  matrix with elements:

$$M_{nn} = \kappa_n - \omega^2 m_n + i\omega b_n \quad ; \quad M_{nj} = \frac{-\omega^2 \rho e^{-ikr_{jn}}}{4\pi r_{jn}} \quad (n \neq j). \tag{9}$$

Each diagonal term (e.g.,  $M_{nn}$ ) describes the resonance behavior of an individual bladder, as if it were uncoupled from all the others. Variations in size, damping, depth etc., may be incorporated into these diagonal elements. Every off-diagonal element (e.g.,  $M_{nj}$ ) describes the radiative coupling between two of the bladders due to their scattered acoustic fields. The matrix falls into two distinct parts. The solution of the matrix equation (i.e.,  $\mathbf{v} = \mathbf{M}^{-1}\mathbf{p}$ ) enables the description of steady state scattering from the whole ensemble of swim bladders as a function of the external field amplitude and frequency. The matrix inversion process incorporates all orders of multiple scattering. Once the solutions  $v_n$  are found for the individual swim bladders, the scattered pressure field for the whole school may be readily obtained using coherent summation.

(3) Time-domain solution for a school: The aim of this research is to obtain explicit analytic time-domain solutions of a more generalized form of equations (8) for arbitrary time-dependent external input fields, i.e.,  $[P_1(t), \dots, P_n(t), \dots, P_N(t)]$ , which are not necessarily harmonic.

The purpose is to then to use these solutions to describe the evolution of sound pulses as they are scattered from, and pass through, fish schools, and to identify discrete segments of the acoustic signal with different sections of the fish school, leading to an improved understanding of signal scattering, signal extinction, and their fluctuations. This is schematically depicted in Figure 1.

## WORK COMPLETED

Work on the project began in March 2011, the beginning of the academic year in Chile. During the period March-October 2011, we have concentrated on using the current steady-state model (Ref. 1) to

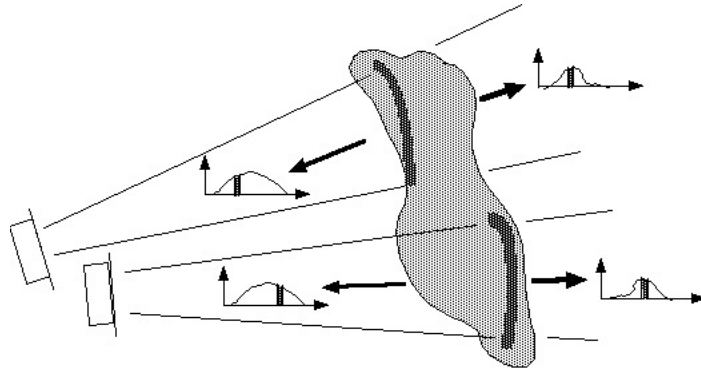


**Figure 1:** *This schematic diagram depicts the concept of identifying individual segments of both the back scattered signal pulse, and that passing through the school, with different sections of the fish school. This should provide a tool for characterizing fluctuations of the acoustic scattering.*

perform a study of the acoustic field in the forward scattering region of a fish school, and to understand how it differs from the back scattered field. In the forward region, the field has two components: the forward scattered field, and the incident field. These usually combine coherently, and it is usually difficult to separate them. The purpose here has been to explore issues which, in the time-domain case, will affect the identification of the forward scattered signal, and the extraction of school information from it.

This aspect of the work has been largely completed, and a paper on it is to be given at the 162nd Meeting of the Acoustical Society of America in San Diego, California 31 October - 4 November 2011.

## RESULTS

Figure 2 shows the target strengths of a small school of fish, as predicted by the school scattering model of Ref. 1. In the upper figure the solid line shows a series of peaks and troughs as a function of frequency, which is characteristic of back scattering from a closely packed school of fish, where the interference effects between the radiated field from the individual fish lead to Bragg scattering effects. The lower figure shows the equivalent target strength in the forward scattering direction, for the same series of random snapshots of 13 fish, assuming no interaction with the incident field. Note, in this case, that the phase differences, which lead to frequency dependent interference effects in the back scattering case, are annulled, so there are no peaks and troughs. The forward scattered fields from the fish are highly coherent. This strongly suggests that, when the time-domain case is addressed, there will likely be similar large differences between the characters of the back and forward scattered fields, which will require different types of interpretation.

The spatial distribution of the ensemble forward scattered field for the 13 fish of Figure 2, is shown in Figure 3. We see that, while scattering from individual fish in the monopole resonance frequency region is practically spherically symmetric, the greater coherence of the scattered fields in the forward scatter direction leads to strongly constructive interference in that direction. However, as we will see, the manifestation of this effect as a detectable phenomenon depends strongly on other factors.

In practice, as mentioned above, the total field in the forward direction is usually formed by the addition of the scattered field and the incident field. In relation to this, another important aspect of scattering in

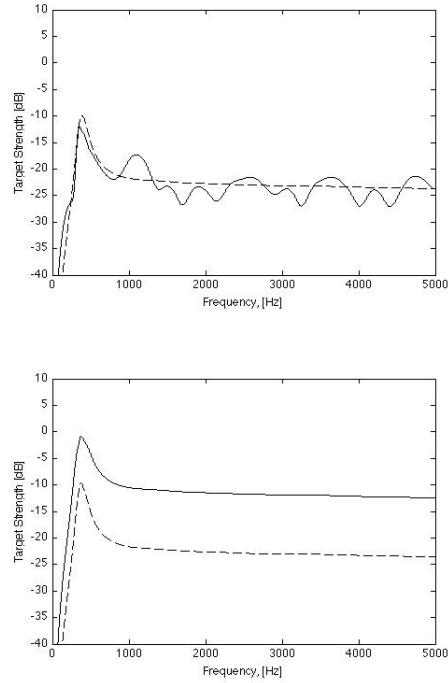


**Figure 2:** *These figures show the target strength predicted for a small school of 13 fish, of average length 40 cm, at a depth of 50 m, with fish flesh viscosity  $\xi = 500$  poise, averaged over ten randomized snapshots of fish locations. In both cases the solid line is the prediction of the school scattering model of Ref. 1, and the dashed line is the target strength of the fish added together incoherently. The upper graph is for back scatter. The lower graph is for forward scatter.*

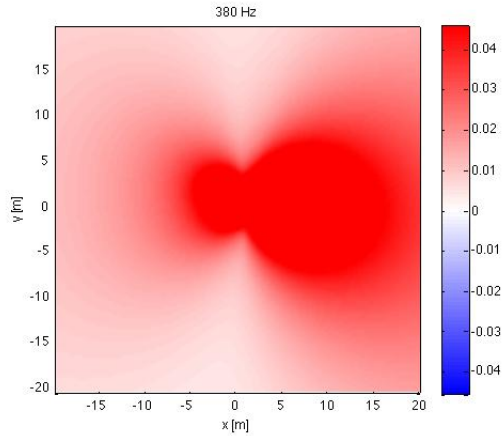


**Figure 3:** *The spatial distribution of the modulus of the scattered field amplitude for the same fish, and series of snapshots, shown in Figure 2. The input field, incident from left to right, is given amplitude 1. The quantity plotted in the figure is  $|p| - 1$ , where  $|p|$  is the scattered field amplitude predicted by the school model. Anything red is  $> 0$ , anything blue is  $< 0$ . The frequency of 380 Hz is the average resonance frequency in the school.*

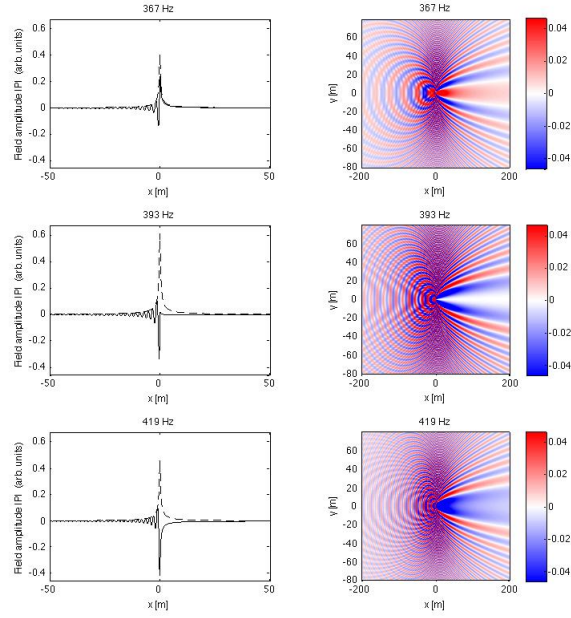


**Figure 4: Combining the scattered field and incident field for a single fish. On the left are plotted the scattered field (dashed line) and total field (solid line), along the  $x$  axis, for excitation of a single bladder of resonance frequency 393 Hz, at three frequencies: 367 Hz, 393 Hz, 419 Hz. On the right are plotted the spatial distributions of the total field amplitude (i.e.,  $|p| - 1$ ) for the same cases. Fish length 40 cm, depth 50 m, fish flesh viscosity  $\xi = 500$  poise.**

the forward direction from fish swim bladders is due to the change of phase introduced by the resonators themselves, which causes the scattered field and the incident field to combine together in different ways, depending upon the applied frequency.

What is seen in Figure 4 is that, when excited below the resonance frequency, the phase of the forward scattered field is such that it interferes constructively with the incident field, to produce a total field amplitude on the forward axis which is greater than that of the incident field. On the other hand, above resonance the fields add destructively, and this leads to a reduction in the total field amplitude below that of the incident field. Exactly at resonance, the total field amplitude is equal to that of the incident field.

In Figure 5, the same quantities (as in Figure 4) are plotted for a large school of 5000 fish. We again see that the phase of the scattered field varies with frequency, such that it interferes with the incident field in variable ways. However, in this case, the effect of incorporating scattering effects from a large ensemble, via the school scattering model, shifts the region where the forward scattered field increases the total field amplitude on the forward axis, to a lower frequency. Even at 200 Hz, which is significantly lower than the resonance frequency, the two fields combine to reduce the amplitude in the forward direction, and therefore the school of fish casts an acoustic “shadow”.

Figure 6 shows the attenuation of the field on the forward axis due to a smaller school of 100 fish, at a range of 5 km. Again, there is no indication of the strong peaks and troughs seen in the back scattering results presented in Figure 2. The average resonance frequency is about 388 Hz, and below this there is a small frequency region where the fields combine to increase the total field amplitude above that of the

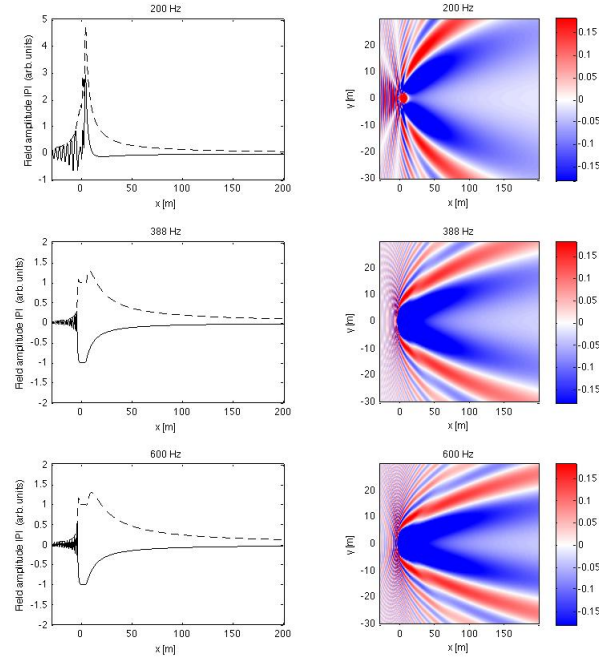


**Figure 5: Combining the scattered field and incident field for a large school of fish. On the left are plotted the scattered field (dashed line) and total field (solid line), along the  $x$  axis, for excitation of the school at three frequencies: 200 Hz, 388 Hz, 600 Hz. On the right are plotted the spatial distributions of the total field amplitude (i.e.,  $|p| - 1$ ) for the same cases. The school has 5000 fish, of average length 40 cm, at a depth of 50 m, with fish flesh viscosity  $\xi = 500$  poise. The average resonance frequency is about 388 Hz.**

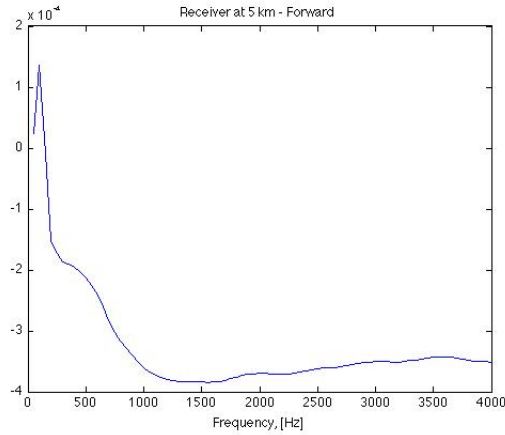


**Figure 6: Attenuation of the acoustic field in the forward direction. The amplitude of the combined acoustic field is plotted (as  $|p| - 1$ ) on the forward axis, as a function of frequency, at a range of 5 km. The school has 100 fish, of average length 40 cm, at a depth of 50 m, with fish flesh viscosity  $\xi = 500$  poise. Results averaged over ten randomized snapshots of fish locations.**



incident field. However, over most of the frequency range, the fish school leads to an attenuation of the acoustic field. This relative pattern of the amplitude distribution is unchanged with distance in the forward direction. The overall amplitude is reduced as distance increases.

## **REFERENCES**

- (1) C. Feuillade, R.W. Nero and R. H. Love, A low frequency acoustic scattering model for small schools of fish, J. Acoust. Soc. Am., **99**, 196-208 (1996).
- (2). R. H. Love, Resonant acoustic scattering by swim bladder-bearing fish, J. Acoust. Soc. Am. **64**, 571-580 (1978).

## **IMPACT/APPLICATIONS**

This work has the potential for indicating how methods of time signal analysis may be used to investigate the stochastic variations of shape and distribution of fish in a school, and how these affect the statistical properties of acoustic scattering from these ensemble objects.

## **TRANSITIONS**

None at the present time.

## **RELATED PROJECTS**

Experimental and other work by other participants in the ONR BRC, Fish Acoustics program.